The Journal of Physiology

An obesogenic diet impairs uncoupled substrate oxidation and promotes whitening of the brown adipose tissue in rats

Daniel Da Eira, Shailee Jani and Rolando B. Ceddia

Muscle Health Research Centre, School of Kinesiology and Health Science, York University, Toronto, Ontario, Canada

Handling Editors: Michael Hogan & Bettina Mittendorfer

The peer review history is available in the Supporting information section of this article (https://doi.org/10.1113/JP283721#support-information-section).

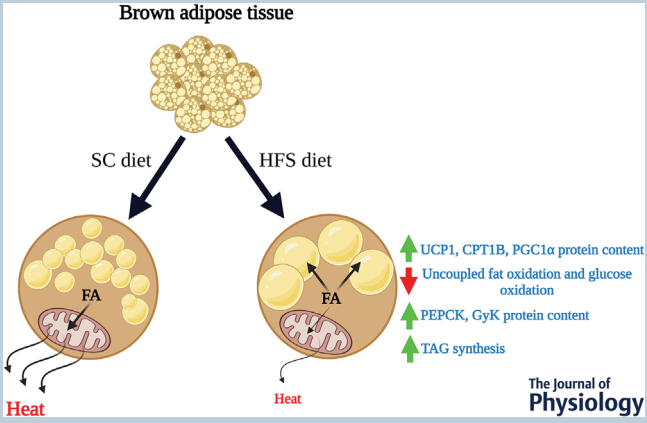

Abstract Brown adipose tissue (BAT) is rich in mitochondria containing uncoupling protein 1 (UCP1), and dissipates energy through thermogenesis. However, even though BAT mass and its UCP1 content increase in rodents chronically fed a high-fat sucrose-enriched (HFS) diet, marked expansion of adiposity still occurs in these animals, suggesting insufficient BAT-mediated HFS diet-induced thermogenesis. Thus, the objective of this study was to investigate the metabolic and molecular mechanisms that regulate BAT thermogenesis in HFS-induced obesity. To accomplish this, rats were fed either a standard chow or HFS diet for 8 weeks. Subsequently, glucose and fatty acid metabolism and the molecular mechanisms underlying these processes were assessed in freshly isolated primary BAT adipocytes. Despite increasing BAT mass and its UCP1 content, the HFS diet reduced uncoupled glucose and palmitate oxidation in BAT adipocytes. It also markedly diminished tyrosine hydroxylase content and lipolysis in these cells. Conversely, glucose uptake, lactate production, glycerol incorporation into lipids, palmitate incorporation into triacylglycerol (TAG), phosphoenolpyruvate carboxykinase and glycerol kinase levels, and lipoprotein lipase and cluster of differentiation 36 gene expression were increased. In summary, a HFS diet enhanced

Daniel Da Eira is a PhD candidate in the School of Kinesiology and Health Science at York University, where he also completed his undergraduate and master's degrees. His Master's research focused on the effects of diet-induced obesity on the thermogenic capacity of brown adipose tissue. As such, he has investigated the mechanisms that regulate fat and glucose metabolism leading to either energy storage or dissipation in brown and beige adipocytes. At present he is completing his doctoral work investigating the impact of a ketogenic diet on the thermogenic machinery in brown and white adipose tissues, as well as the influence of this diet on components of the renin–angiotensin system in brown and white fat.

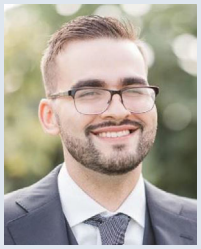

DOI: 10.1113/JP283721

glyceroneogenesis and shifted BAT metabolism toward TAG synthesis by impairing UCP1-mediated substrate oxidation and by enhancing fatty acid esterification in intact brown adipocytes. These adaptive metabolic responses to chronic HFS feeding attenuated BAT thermogenic capacity and favoured the development of obesity.

(Received 10 August 2022; accepted after revision 9 November 2022; first published online 23 November 2022)
Corresponding author R. B. Ceddia: Muscle Health Research Center, School of Kinesiology and Health Science, York University, 4700 Keele St, North York, ON M3J 1P3, Canada. Email: roceddia@yorku.ca

Abstract figure legend In brown adipocytes from lean rats fed a standard laboratory chow (SC) diet, glucose and fatty acids (FA) were diverted essentially toward uncoupling protein 1 (UCP1)-mediated substrate oxidation and thermogenesis. Conversely, in brown adipose tissue (BAT) of rats fed a high-fat sucrose-enriched (HFS) obesogenic diet, despite increases in UCP1, carnitine palmitoyltransferase 1B (CPT1B), and peroxisome proliferator-activated receptor γ coactivator 1α (PGC-1α) contents, substrate metabolism was shifted toward triacylglycerol (TAG) synthesis/storage. This was characterized by reduced UCP1-mediated glucose and fatty acid oxidation. These adaptive responses to a chronic HFS diet were supported by increased contents of phosphoenolpyruvate carboxykinase (PEPCK) and glycerol kinase (GyK).

Key points

- Despite increasing brown adipose tissue (BAT) mass and levels of thermogenic proteins such as peroxisome proliferator-activated receptor γ coactivator 1α, carnitine palmitoyltransferase 1B and uncoupling protein 1 (UCP1), an obesogenic high-fat sucrose-enriched (HFS) diet attenuated uncoupled glucose and fatty acid oxidation in brown adipocytes.
- Brown adipocytes diverted glycerol and fatty acids toward triacylglycerol (TAG) synthesis by elevating the cellular machinery that promotes fatty acid uptake along with phosphoenolpyruvate carboxykinase and glycerol kinase levels.
- The HFS diet increased glucose uptake that supported lactate production and provided substrate for glyceroneogenesis and TAG synthesis in brown adipocytes.
- Impaired UCP-1-mediated thermogenic capacity and enhanced TAG storage in BAT adipocytes were consistent with reduced adipose triglyceride lipase and tyrosine hydroxylase levels in HFS diet-fed animals.

Introduction

Despite variations in the availability of food/energy, body weight can be maintained relatively constant over long periods of time (Rosenbaum & Leibel, 1998). This is possible because under conditions of food abundance and overeating, the organism activates mechanisms that promote energy dissipation and attenuate weight gain. Conversely, under conditions of food scarcity and reduced intake, energy-sparing mechanisms are activated and oppose weight loss (Leibel, 2008; Trayhurn, 2017). These adaptive metabolic responses are referred to as diet-induced thermogenesis (DIT), and play an important role in regulating body weight and whole-body energy homeostasis (Trayhurn, 2017). The ability to dissipate energy under conditions of overeating has been, at least partially, attributed to sympathetic nervous system (SNS)-mediated activation of brown adipose tissue (BAT) (Trayhurn, 2017). This is because uncoupling protein 1 (UCP1) uncouples oxidative phosphorylation from ATP synthesis, resulting in the production of heat in a process known as non-shivering thermogenesis (NST) (Barbara & Nedergaard, 2004; Kozak, 2010; Trayhurn, 2017). This process is triggered by the release of noradrenaline that binds to β-adrenergic receptors on brown adipocytes and promotes lipolysis within the cells. The release of fatty acids (FA) then leads to the activation of UCP1 that ultimately promotes mitochondrial uncoupling and NST in BAT adipocytes (Barbara & Nedergaard, 2004; Fedorenko et al., 2013).

A role for BAT in DIT is supported by studies demonstrating that the mass of this tissue expands and its UCP1 content increases under diet-induced obesity (DIO) conditions in rats (So et al., 2011; Wu et al., 2014), and also by the fact that UCP1 ablation causes obesity in mice living at thermoneutrality (Feldmann et al., 2009). However, despite evidence of tissue enlargement and increased UCP1 content in BAT, great expansion of adiposity still occurs in animals subject to DIO (So et al., 2011; Wu et al.,

2014). This suggests that NST is either insufficient to offset the energy surplus or that it might even be suppressed under conditions of chronic overeating. In both cases the magnitude of energy dissipation through NST in BAT would be limited, allowing for extensive growth of the white adipose tissue (WAT) to occur. In this context, we have found that in the first and second weeks of feeding rats *ad libitum* a high-fat sucrose-enriched (HFS) diet, whole-body energy expenditure increased by ∼14 and 11%, respectively, in comparison to standard laboratory chow (SC) diet-fed controls (So et al., 2011). However, as HFS feeding continued through six additional weeks, whole-body energy expenditure no longer differed from that of SC diet fed rats (So et al., 2011), suggesting that an initial thermogenic response was mounted, but it was not sustained in rats chronically exposed to a HFS diet. Thus, it could be that NST in BAT was suppressed in a time-dependent manner, even though expansion of tissue mass and its UCP1 content persisted with continued overfeeding. This is consistent with recent human studies using ^{18}F-labelled fluorodeoxyglucose positron emission tomography–computed tomography to measure BAT volume and its activity in lean and obese subjects (Leitner et al., 2017). In fact, it has been reported that after 5 h of tolerable cold exposure (16°C), activated BAT in obese men corresponded to only ∼39% of that of lean counterparts, even though the total volume of BAT-containing depots was almost two-fold higher in the former than the latter group of subjects (Leitner et al., 2017). Thus, it was clear that BAT mass was increased in obese subjects, whereas its recruitment for thermogenesis was not (Leitner et al., 2017). We have previously reported that the HFS diet-induced increase in BAT UCP1 levels was accompanied by increased rates of fatty acid oxidation in homogenized BAT samples (So et al., 2011; Wu et al., 2014). This was consistent with an enhanced machinery that consumes substrate under conditions of activated NST. However, any regulatory mechanisms that could potentially regulate substrate consumption in BAT adipocytes was lost in tissue homogenates. It could be that, in intact BAT adipocytes, cellular regulatory mechanisms shift the flux of substrate toward pathways that promote storage as opposed to energy dissipation. This could help explain why increased BAT tissue mass and UCP1 levels do not prevent adipose tissue expansion in rodents and humans under conditions of DIO. In this context, the objective of this study was to investigate the molecular and metabolic mechanisms that regulate DIT in BAT under conditions of DIO and identify alterations in substrate flux that could lead to fat accumulation instead of energy dissipation. To this end, rats were fed either a SC or a HFS diet for 8 weeks. Subsequently, glucose and fat metabolism and the molecular mechanisms underlying these processes were assessed in freshly isolated intact BAT adipocytes. A detailed assessment of the metabolic pathways that regulate energy storage and dissipation in BAT adipocytes was performed. We found that despite increased tissue mass and UCP1 content in BAT, chronic exposure to a HFS diet reduced UCP1-mediated glucose and fat oxidation, attenuated lipolysis and shifted metabolism towards TAG synthesis/storage in intact brown adipocytes. Altogether, these molecular and metabolic changes induced by chronic exposure to an obesogenic HFS diet contributed to lower uncoupled substrate oxidation in BAT and favoured the development of obesity.

Methods

Ethical approval

The investigators understand the ethical principles under which *The Journal* operates and their work complies with *The Journal*'s animal ethics checklist. The protocol containing all animal procedures described in this study was specifically approved by the Committee on the Ethics of Animal Experiments of York University (York University Animal Care Committee, YUACC, permit number: 2021-03) and was performed strictly in accordance with the YUACC guidelines. All tissue extraction procedures were performed under ketamine/xylazine anaesthesia (90 mg and 10 mg/100 g body weight, respectively), and all efforts were made to minimize suffering. Upon completion of tissue extraction, all animals were decapitated. All experiments in this study were carried out in compliance with the ARRIVE guidelines.

Reagents

Type II collagenase, isoproterenol, FA-free bovine serum albumin (BSA), palmitic acid, and the free glycerol determination kit were purchased from Sigma (St Louis, MO, USA). Oligomycin was purchased from Cayman Chemical (Ann Arbor, MI, USA). [1-^{14}C]Palmitic acid, [U-^{14}C]glycerol and D-[U-^{14}C]glucose were purchased from American Radiolabelled Chemicals (St Louis, MO, USA). The lactate assay kit was from BioVision (Milpitas, CA, USA). Protease (cOmplete Ultra Tablets) and phosphatase (PhosSTOP) inhibitors were obtained from Roche Diagnostics GmbH (Mannheim, Germany). β-Actin (cat. no. 4967), tyrosine hydroxylase (TH; cat. no. 2792), adipose triglyceride lipase (ATGL; cat. no. 2138), hormone-sensitive lipase (HSL; cat. no. 4107), and pHSL$_{Ser660}$ (cat. no. 4126) antibodies were purchased from Cell Signaling Technology (Danvers, MA, USA). β_3-adrenergic receptor (β_3-AdR, cat. no. sc-50 436) and glucose transporter 4 (GLUT4, cat. no. sc-7938) antibodies were purchased from Santa Cruz Biotechnology (Dallas, TX, USA). Carnitine palmitoyltransferase 1B

(CPT1B, cat. no. PB9491) antibody was purchased from BosterBio (Pleasanton, CA, USA). Glucose transporter 1 (GLUT1, cat. no. ab115730), glycerol kinase (GYK) (cat. no. ab180525), phosphoenolpyruvate carboxykinase cytoplasmic (PEPCK-C, cat. no. ab28455), and uncoupling protein 1 (UCP1, cat. no. ab23841) were purchased from Abcam (Toronto, ON, Canada). Peroxisome proliferator-activated receptor γ coactivator-1α (PGC-1α, cat. no. AB3242) antibody was purchased from Millipore (Temecula, CA, USA).

Animals and diet

Male albino rats (Wistar strain) at approximately 250 g were group-housed at 22°C on a 12/12-h light–dark cycle. These rats were assigned to either a standard laboratory chow (SC) diet (27% protein, 13% fat and 60% carbohydrates from Test Diet cat. no.5012, Richmond, IN, USA) group or a high-fat sucrose-enriched (HFS) diet (20% protein, 60% fat (laird/soybean oil), 20% carbohydrates (sucrose); from Research Diets, cat. no. D12492, New Brunswick, NJ, USA) group and were fed *ad libitum* for 8 weeks. After 8 weeks of feeding, animals were anaesthetized and tissues were harvested for experiments.

Body weight and fat mass

Changes in body weight were measured by comparing weekly weight recordings to a baseline measurement. Interscapular brown adipose tissue (iBAT), aortic BAT (aBAT), subcutaneous inguinal (Sc Ing), and epididymal (Epid) fat pads were extracted, trimmed of any non-fat tissue and individually weighed.

Brown adipose tissue extraction and brown adipocyte isolation

iBAT and aBAT were extracted and carefully trimmed of any muscle, connective tissue and white fat and used for adipocyte isolation as previously described (Cannon & Nedergaard, 2001). iBAT and aBAT were combined to maximize the yield of brown adipocytes. The tissues were initially incubated in Krebs–Ringer bicarbonate HEPES (KRBH) buffer prepared fresh on the day of each experiment from stock solutions of salts and buffers (stored at 4°C) to give the following final concentrations: 120 mM NaCl, 4.8 mM KCl, 2.5 mM $CaCl_2$, 1.2 mM KH_2PO_4, 1.2 mM $MgSO_4$, 15 mM $NaHCO_3$ and 30 mM HEPES. The solution was gassed for 45 min with carbogen (95% O_2, 5% CO_2) and then bovine serum albumin (4%) and glucose (5.5 mM) were added. The pH of the buffer was adjusted to 7.4 with NaOH before use. Subsequently, the combined tissues were vortexed for 5 s and filtered, with the filtrate being discarded. The remaining tissues were finely minced and incubated in fresh KRBH–4% BSA containing collagenase (0.83 mg ml^{-1}) at 37°C under orbital agitation (120 orbital strokes/min) for about 20–30 min. The digested tissue was then strained using a nylon mesh and isolated cells were transferred to plastic tubes, washed three times, and resuspended in KRBH containing 3.5% FA-free BSA (KRBH–3.5% BSA). In order to distribute an equal number of adipocytes in each treatment condition, cell diameters were measured and total cell counts were determined (Fine & DiGirolamo, 1997).

Glucose and palmitate oxidation

Glucose and palmitate oxidation as a measure of oxidative capacity were assessed by $^{14}CO_2$ release in isolated BAT adipocytes (5×10^5 cells) as previously described (Gaidhu et al., 2011). Adipocytes were incubated in KRBH–3.5% BSA containing either 0.2 μCi ml^{-1} of [1-^{14}C]palmitic acid and 200 μM non-labelled palmitate, or 0.2 μCi ml^{-1} of D-[U-^{14}C]glucose and 5.5 mM non-labelled D-glucose for 1 h. To examine the effect of lipolysis on substrate oxidation, the β-agonist isoproterenol (Iso, 100 nM) was added to the medium. To distinguish substrate oxidation for ATP production (coupled respiration) from UCP1-mediated proton leak (uncoupled respiration), the ATP synthase inhibitor oligomycin (Oligo, 100 μM) was added to cells 15 min prior to the incubation in the absence or presence of Iso. Following the 1 h incubation period, the media were acidified using 0.2 ml of H_2SO_4 (5 M) and kept sealed for one additional hour for the release and collection of $^{14}CO_2$ from the cells and media. The incubation vials were prepared with a centred well containing a filter paper that was moistened with 0.2 ml of 2-phenylethylamine–methanol (1:1, v:v) for the capture of $^{14}CO_2$. At the end of the incubation, the filter paper was removed from the well and placed in scintillation fluid for radioactive counting (Gaidhu et al., 2009, 2010).

Lipolysis

Lipolysis was measured in isolated BAT adipocytes (7.5×10^5 cells). Each assay was conducted in triplicate and samples were incubated for 75 min at 37°C with gentle shaking (50 orbital strokes/min). Following the incubation, a 200 μl aliquot of the incubation medium was extracted from each vial for the determination of glycerol concentration.

Glycerol incorporation into lipids and palmitate incorporation into TAG

Glycerol incorporation into lipids and palmitate incorporation into TAG were measured using isolated BAT adipocytes (5×10^5 cells). Adipocytes were

incubated in KRBH–3.5% BSA containing 0.2 μCi ml^{-1} of [U-^{14}C]glycerol for 1 h. Subsequently, lipid extraction took place according to the method of Dole & & Meinertz (1960) and counted for radioactivity (Gaidhu et al., 2009). Palmitate incorporation into TAG was measured in isolated BAT adipocytes (5 × 10^5 cells) incubated in KRBH–3.5% BSA containing 0.2 μCi ml^{-1} of [1-^{14}C]palmitic acid and 200 μM non-labelled palmitate for 1 h. Lipids were extracted from these adipocytes using Folch's method (Folch et al., 1957), dried under nitrogen, and resuspended in 50 μl of chloroform:methanol (2:1, v:v). Four microlitres of sample and TG standard (triolein, Nu-Chek Prep Inc., Elysian, MN, USA) were spotted 2 cm above the lower edge of silica coated flexible polyester thin layer chromatography plates (20 cm × 20 cm) (Whatman, Maidstone, UK). Lipids were separated using a hexane–diethyl ether–acetic acid (70:30:1, v:v:v) solvent and then exposed to iodine vapour for visualization. After the evaporation of iodine, the spots adjacent to the standard, corresponding to TG, were scraped off the plate and counted for radioactivity.

Glucose uptake

Isolated adipocytes were used to determine glucose uptake as described previously (Gaidhu et al., 2006). Briefly, adipocytes were resuspended in glucose-free KRB containing HEPES (30 mM; KRB-HEPES) and 1% BSA, pH 7.4. Subsequently, 1 × 10^6 cells were transferred to plastic tubes and incubated at 37°C for 1 h. Insulin (100 nM) was added for the final 20 min of the incubation period. Subsequently, KRB-HEPES containing 0.5 mM 2-deoxy-D-glucose and 0.5 μCi of 2-[1,2-^{3}H]deoxy-D-glucose was added to the cells for 3 min, and the incubations were terminated by the addition of cytochalasin B (1.5 mM stock solution). Aliquots of cell suspension (240 μl) were quickly placed in plastic microtubes containing 100 μl of di-'isononyl' phthalate. The tubes were centrifuged for 30 s (6000 *g*) to separate cells from the radioactive incubation medium. Subsequently, fat cells were collected by cutting the tubes through the oil phase and transferred to scintillation vials to be counted for radioactivity. Radioactivity of the cells unrelated to glucose transport (nonspecific transport) was determined in the same conditions by adding cytochalasin B (50 μM final concentration) to the medium before the addition of cells (Gaidhu et al., 2006). Non-specific values were subtracted from all conditions.

Measurement of lactate production

Lactate production was measured using a commercially available kit (BioVision; Milpitas, CA, USA) as per the manufacturer's instructions. Briefly, cells were isolated as described above and incubated in KRBH–3.5% BSA for 75 min. Following incubation, an aliquot of medium was extracted and stored at −80°C until analysis.

RNA isolation and quantitative PCR

BAT samples were flash-frozen in liquid nitrogen and stored at −80°C until RNA isolation. RNA was isolated using TRIzol^{TM} (Thermo Fisher Scientific, Waltham, MA, USA) and complimentary DNA (cDNA) was made with 2 μg of RNA using ABM EasyScript^{TM} Reverse Transcriptase cDNA Synthesis kit (Diamed, Mississauga, ON, Canada) as per the manufacturer's instructions. Primers were designed using the software PrimerQuest (IDT) based on probe sequences available at the Affymetrix database (NetAffx^{TM} Analysis Center, http://www.affymetrix.com/ analysis) for each given gene. Samples were run in duplicate on a 96-well plate. Each 20 μl reaction contained 4 μl of cDNA, 0.4 μl of primer, 10 μl of Brightgreen 2× qPCR Mastermix (Diamed) and 5.6 μl of RNase-free water. qPCR analysis was performed using a Bio-Rad CFX96 Real Time PCR Detection System (Bio-Rad, Mississauga, ON, Canada) using the following amplification conditions: 95°C (10 min); 40 cycles of 95°C (15 s), 60°C (1 min). All genes were normalized to the housekeeping-gene β-actin, and relative differences in gene expression between treatment groups were determined using the $\Delta\Delta C_t$ method (Livak & Schmittgen, 2001). Values are presented as fold increases relative to the SC group. The primers used were as follows: cluster of differentiation 36 (*Cd36*) forward (ACGACTGCAGGTCAACATACTGGT), reverse (TGGTCCCAGTCTCATTTAGCCACA); lipoprotein lipase (*Lpl*) forward (TTGAGAAAGGG CTCTGCCTGAGTT), reverse (TGCTTCTCTTGGCTC TGACCTTGT).

Western blotting

BAT samples were extracted from each rat, snap-frozen in liquid nitrogen and frozen at −80°C for later use. Tissues were homogenized in buffer containing 25 mM Tris–HCl, 25 mM NaCl (pH 7.4), 1 mM $MgCl_2$, 2.7 mM KCl, 1% Triton X-100 and protease and phosphatase inhibitors (Roche Diagnostics). Following centrifugation of the homogenates, the infranatant was collected. An aliquot of each sample was used in a Bradford assay to determine protein concentration. The samples were then diluted 1:1 with 2× Laemmli sample buffer and incubated at 95°C for 5 min. Twenty-five micrograms of protein from each sample was loaded onto gels and subject to SDS-PAGE, transferred to a polyvinylidene difluoride membrane and probed with the antibody of interest. The antibody dilutions were 1:1000 and the loading control

Table 1. Cumulative weight gain of rats fed either standard chow (SC) or a high-fat sucrose-enriched (HFS) diet for 8 weeks

	Cumulative weight gain (g)							
Group	1 week	2 weeks	3 weeks	4 weeks	5 weeks	6 weeks	7 weeks	8 weeks
SC	31.2 ± 3.8	68.5 ± 18.6	103.1 ± 31.9	127.8 ± 44.3	151.0 ± 54.7	167.8 ± 61.9	187.6 ± 62.1	210.0 ± 69.0
HFS	41.5 ± 14.4	101.8 ± 17.4	149.6 ± 19.9	188.6* ± 25.8	223.2* ± 33.8	254.3* ± 38.3	283.2* ± 41.3	314.2* ± 44.0

*$P < 0.05$ *vs.* SC. Repeated measures two-way ANOVA was used to compare groups/weeks. $n = 10–13$ rats.

was β-actin. Densitometry analysis was conducted using the Scion Image program.

Adipose tissue morphology

Morphological analysis of iBAT was performed using light microscopy as described previously (Gaidhu et al., 2011; Wu et al., 2014). Briefly, a sample (∼50−100 mg) of each fat tissue was collected and fixed in 4% paraformaldehyde, 0.1 M phosphate-buffered saline (PBS), pH 7.4, for 24 h at room temperature. Following fixation, adipose tissue samples were washed three times in PBS and stored at 4°C in 70% ethanol. Samples were then embedded in paraffin blocks, sectioned, and stained with haematoxylin and eosin (H & E). Digital images of tissue sections were captured with a Nikon Eclipse Ti (Nikon Canada, Mississauga, ON, Canada) under ×20 and ×40 magnification.

Statistical analysis

Statistical analyses were conducted by using either Student's unpaired *t* test or ANOVA with the Bonferroni *post hoc* comparison using the GraphPad Prism statistical analysis program (GraphPad Software Inc., San Diego, CA, USA). Tests for normality of the distribution were performed using the D'Agostino–Pearson test, Anderson–Darling test, Shapiro–Wilk test and Kolmogorov–Smirnov test. All statistical analyses were conducted using GraphPad Prism. Data are expressed as mean ± SD.

Results

Effects of HFS feeding on body weight, fat mass and BAT adipocyte morphology

To confirm that obesity was induced by a HFS diet, we measured weight gain relative to baseline and adipose tissue mass throughout the feeding period. The weight gained in weeks 1−3 was not statistically significantly different from the SC groups, although the average weight gained in the HFS group was higher in each of these weeks. After week 4, the weight gained in the HFS group was significantly higher than in the SC animals (188.6 ± 25.8 *vs.* 127.8 ± 44.3 g) (Table 1). This difference in weight gain persisted until the end of the study, culminating with HFS rats gaining ∼50% more weight than SC controls after 8 weeks of feeding. Differences in weight gain were essentially due to enhanced growth of the WAT in the HFS animals because the masses of the Sc Ing and Epid fat pads in HFS rats were 2.6- and 3-fold larger, respectively, than those of SC controls (Fig. 1*A*). Similarly, iBAT and aBAT masses both increased 1.6-fold in the HFS animals (Fig. 1*B*). Furthermore, H&E staining revealed that iBAT from SC rats contained adipocytes that were essentially multilocular, whereas iBAT from HFS rats contained many cells of unilocular appearance (Fig. 1*C*).

Effects of HFS feeding on PGC-1α, CPT1B and UCP1 contents

After observing an increase in BAT mass, it was important to determine whether this was accompanied by an increase in thermogenic proteins. Indeed, animals in the HFS group exhibited 1.65-, 17- and 2.2-fold increases in protein content of PGC-1α (Fig. 1*D*), CPT1B (Fig. 1*E*), and UCP1 (Fig. 1*F*), respectively, relative to the control group. Taken together, these results indicate that the molecular machinery necessary for oxidation and thermogenesis was enhanced in BAT under conditions of DIO.

Effects of isoproterenol and oligomycin on glucose and palmitate oxidation in BAT adipocytes

To test whether the increased content of thermogenic proteins was accompanied by enhanced substrate oxidation in BAT adipocytes, we measured glucose and palmitate oxidation in these cells. Measurements were conducted under basal conditions as well as in the presence of the β-adrenergic stimulator isoproterenol (Iso) and of the ATP synthase inhibitor oligomycin (Oligo). We found that rates of glucose oxidation in BAT adipocytes from SC and HFS rats were not affected by incubation with either Iso or Oligo or by a combination of both agents (Fig. 2*A*). However, the rates of glucose oxidation in adipocytes from HFS rats

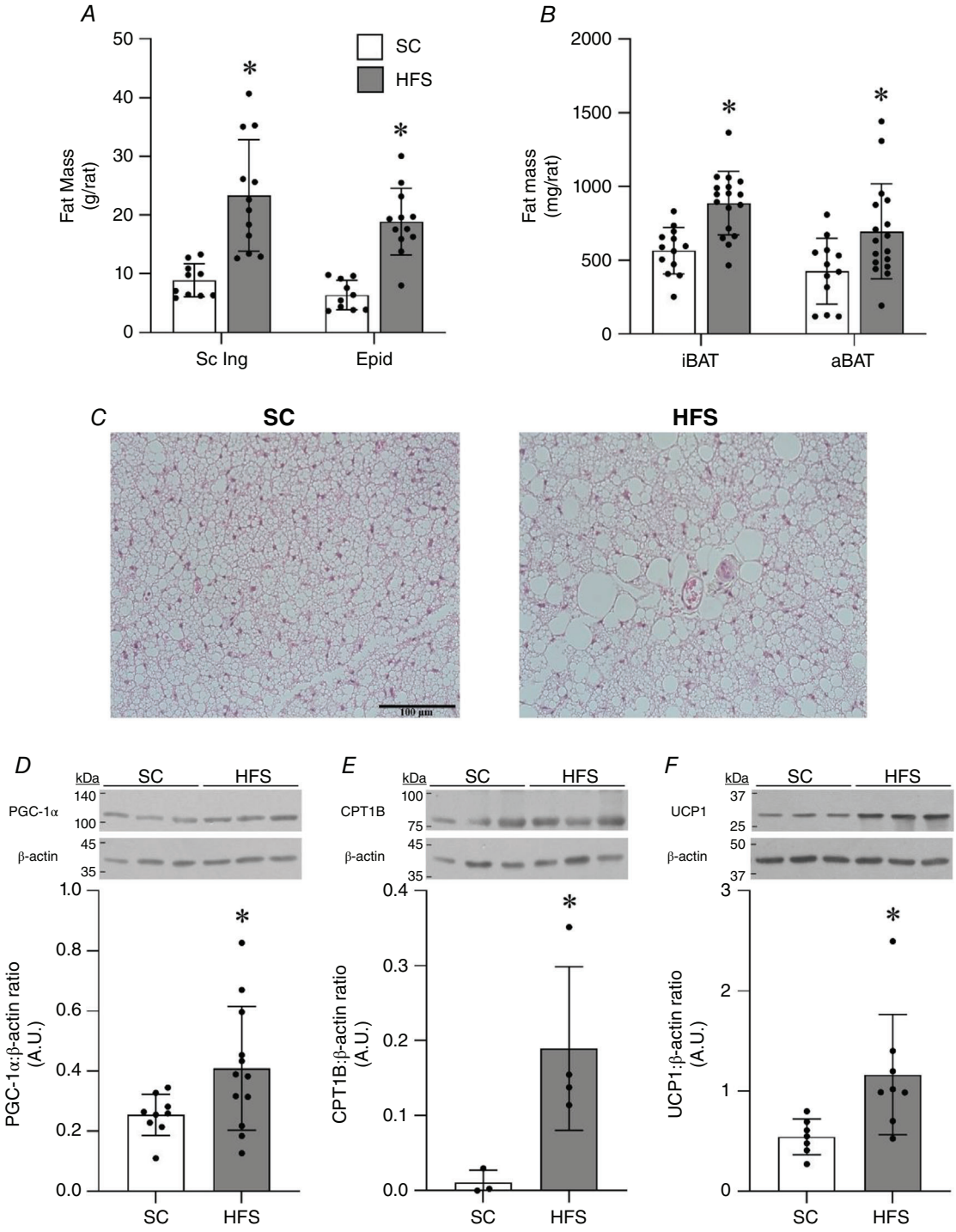

Figure 1. HFS diet increases the masses of white (*A*) and brown (*B*) adipose tissues, the unilocular appearance of brown adipocytes (*C*), and the contents of PGC-1α (*D*), CPT1B (*E*) and UCP1 (*F*) in brown adipose tissue

Data are means ± SD; n = 3–15 rats.*$P < 0.05$ *vs*. SC. Student's t test was used to compare differences between groups in *A*, *B* and *D*–*F*. [Colour figure can be viewed at wileyonlinelibrary.com]

trended to decrease under all conditions investigated, and reached statistical significance under Oligo conditions. In fact, glucose oxidation under basal conditions was 48% lower in BAT adipocytes from HFS- than from SC-fed rats (Fig. 2*A*). Similarly, rates of glucose oxidation in the presence of either Iso or Oligo or Iso+Oligo were 49%, 62% and 57% lower in HFS than SC BAT adipocytes, respectively (Fig. 2*A*). The incubation of BAT adipocytes with Oligo did not reduce glucose oxidation relative to basal conditions, which is consistent with mitochondrial uncoupling accounting for most of the glucose being oxidized in both SC and HFS cells. We then assessed the oxidation rates of fatty acids, which are major thermogenic substrates in brown adipocytes (Barbara & Nedergaard, 2004). Under basal conditions, palmitate oxidation did not differ between the SC and HFS groups (Fig. 2*B*). However, in the presence of Oligo, palmitate oxidation significantly increased by 2.7-fold in BAT adipocytes compared with SC-fed animals, whereas in BAT adipocytes from HFS animals, Oligo did not cause any alteration in this parameter (Fig. 2*B*) in comparison to basal values. Therefore, when comparing rates of palmitate oxidation between SC BAT and HFS BAT adipocytes incubated with Oligo, we found it to be 57% lower in the latter than the former cells (Fig. 2*B*). Furthermore, when incubated with both Iso and Oligo, palmitate oxidation was reduced by 45% in the brown adipocytes of the HFS group (Fig. 2*B*), although this was not statistically significant. These findings demonstrated that UCP1-mediated palmitate oxidation was impaired under conditions of chronic HFS feeding.

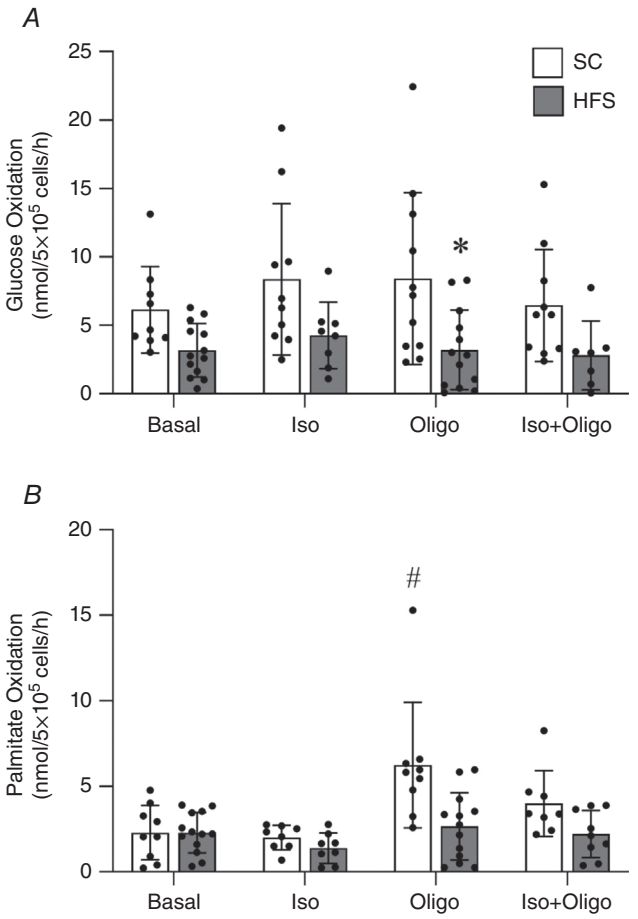

Figure 2. Isolated brown adipocytes from rats fed a HFS diet displayed reduced rates of Oligo-induced glucose (*A*) and palmitate oxidation (*B*) in isolated brown adipocytes
Data are means ± SD; n = 7–13 rats. Two-way ANOVA was used to compare groups/conditions. $^{*}P < 0.05$ *vs.* SC; $^{\#}P < 0.05$ *vs.* all conditions except SC Iso+Oligo.

Effects of HFS feeding on glucose uptake, lactate production, and GLUT1 and GLUT4 protein contents in isolated brown adipocytes

Given that rates of glucose oxidation were reduced in HFS BAT adipocytes, we conducted additional experiments to assess whether the uptake of glucose was also affected in these cells. It could be that low rates of glucose oxidation were driven by reduced intake of this substrate. However, we found that basal glucose uptake in HFS BAT adipocytes was 4-fold higher than in SC BAT adipocytes. In the presence of insulin, SC BAT adipocytes displayed a 4-fold increase in glucose uptake, whereas HFS BAT adipocytes increased glucose uptake 1.83-fold when stimulated with insulin (Fig. 3*A*). Nevertheless, insulin-stimulated glucose uptake was higher in the brown adipocytes of HFS-fed animals than in the SC animals (Fig. 3*A*). To further investigate the metabolic fate of glucose, we measured lactate production in isolated BAT adipocytes and found that, under basal conditions, cells from HFS animals produced 2.7-fold more lactate than adipocytes from SC-fed animals (Fig. 3*B*). These effects of HFS adipocytes were accompanied by a significant increase of ∼24-fold in GLUT1 (Fig. 3*C*) and no alteration in GLUT4 protein contents in iBAT (Fig. 3*D*). Taken together, these findings provide evidence that a HFS diet enhances glucose uptake and shifts glucose metabolism toward lactate production in BAT adipocytes.

Glycerol incorporation into lipids and palmitate incorporation into TAG in brown adipocytes

Because an increased number of unilocular adipocytes was found within BAT from HFS rats, we then measured pathways involved in TAG synthesis. We found that a HFS diet enhanced glycerol incorporation into lipids (Fig. 4*A*) and palmitate incorporation into TAG (Fig. 4*B*) by 1.8- and 1.7-fold, respectively, in BAT adipocytes. This indicated that fatty acids and glycerol were indeed diverted

by chronic HFS feeding towards esterification in isolated BAT adipocytes.

PEPCK and GyK protein levels and *Lpl* and *Cd36* gene expression in BAT

PEPCK (Fig. 4*C*) and GyK (Fig. 4*D*) increased 1.8- and 2.1-fold, respectively, which was accompanied by increases of 3.6-fold in *Lpl* and 3.7-fold in *Cd36* mRNA expression in BAT (Fig. 4*E*). Therefore, our findings provide evidence that the molecular machinery that supports TAG storage was enhanced in BAT by a chronic HFS diet.

Lipolysis, β3-AdR, TH, ATGL and pHSL contents in BAT

Basal lipolysis was reduced by 65% in BAT adipocytes from HFS rats in comparison to the SC group (Fig. 5*A*). Western blot analysis of the molecular machinery involved in lipolysis revealed that ATGL content was significantly reduced by 28% (Fig. 5*B*), whereas HSL_{660} phosphorylation was increased under conditions of HFS feeding, although not statistically significant (Fig. 5*C*). Furthermore, the contents of TH (Fig. 5*D*) and β3AdR (Fig. 5*E*) were reduced and increased by 84% and 6-fold, respectively, in BAT of HFS rats in comparison to SC controls. Based on these findings, it was evident that the observed downregulation of lipolysis in HFS BAT adipocytes derived from distinct alterations in the lipolytic machinery.

Discussion

Here, we provide evidence that UCP1-mediated glucose and fatty acid oxidation in intact and freshly isolated rat brown adipocytes is reduced under conditions of chronic HFS feeding, even though BAT mass and its UCP1 content increased. These findings are consistent with an adaptive response of the organism to the HFS diet that led to attenuation of DIT and expansion of WAT mass. Moreover, BAT itself developed functional and morphological characteristics that resemble WAT, which was characterized by brown adipocytes enhancing their ability to store TAG and by increasing the number

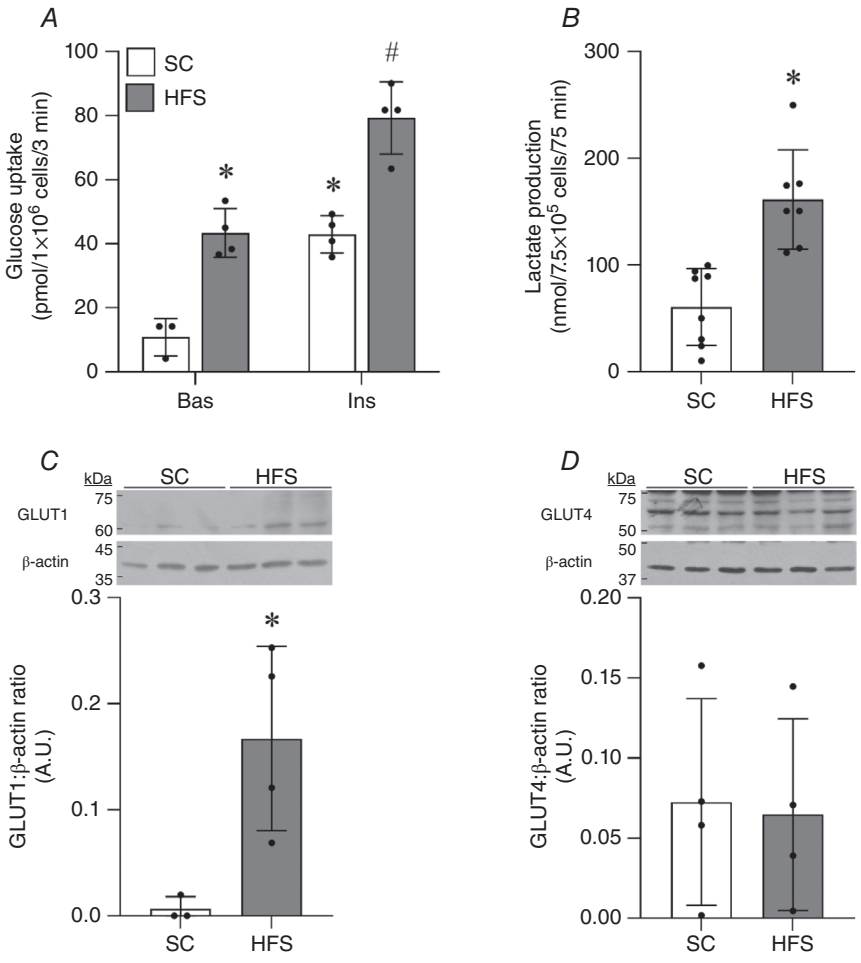

Figure 3. HFS feeding increased basal and insulin-stimulated glucose uptake (*A*), and lactate production (*B*) in isolated BAT adipocytes. HFS also had higher GLUT1 content (*C*) than standard chow (SC) BAT, whereas GLUT4 content (*D*) did not differ between SC and HFS BAT
Data are means ± SD; n = 3–9 rats. $^{\#}P < 0.05$ *vs.* HFS Basal and SC Ins in A. $^{*}P < 0.05$ *vs.* SC Basal in *A*. $^{*}P < 0.05$ *vs.* SC in *B–D*. Student's t test was used to compare groups except for glucose uptake (*A*) where a two-way ANOVA was used to compare groups/conditions.

of cells displaying a unilocular appearance within BAT. The mechanisms underlying these adaptive responses of BAT to HFS-induced obesity involved a major shift in brown adipocyte metabolism. Lipolysis was suppressed and glucose and FA were essentially diverted away from oxidation and toward pathways that culminated in TAG synthesis and enlargement of the lipid droplet in HFS BAT adipocytes (Fig. 6). Thus, our data provide evidence that there are regulatory mechanisms in intact brown adipocytes cells that shift substrate partitioning in response to alterations in dietary macronutrient composition. In this context, we demonstrated that UCP1-mediated mitochondrial uncoupling was impaired under conditions of DIO, confirming our original hypothesis.

It is well established that when BAT is in its activated state (e.g. cold exposure and β3-adrenergic stimulation), the uptake and utilization of glucose by brown adipocytes are enhanced (Barbara & Nedergaard, 2004; Labbe et al., 2015; Olsen et al., 2017). Thus, we expected that DIT in response to the HFS diet would elicit a similar effect in BAT adipocytes. However, given that previous studies

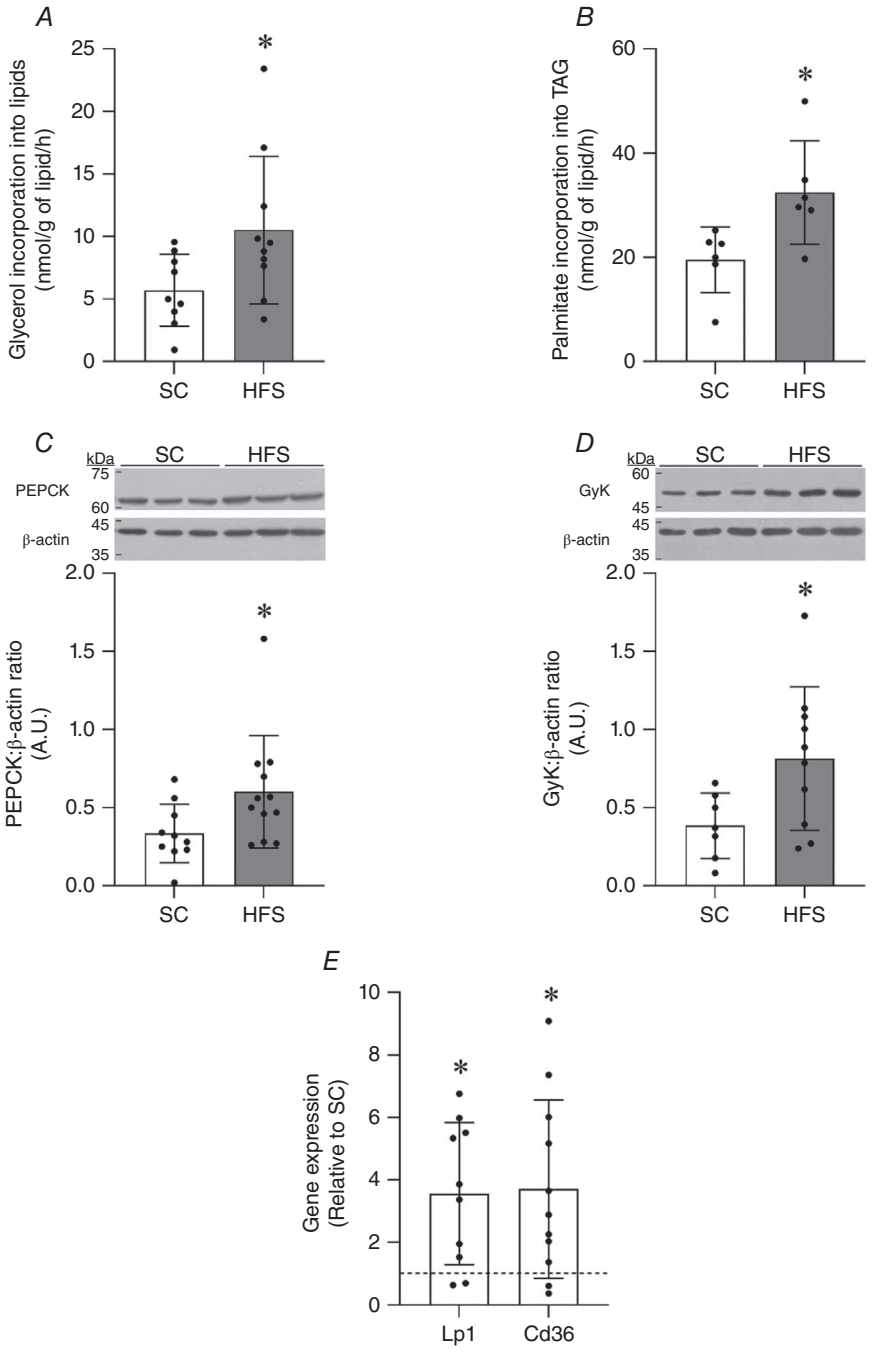

Figure 4. HFS feeding enhanced the incorporation of glycerol into lipids (*A*) and palmitate into triacylglycerol (TAG) (*B*) in isolated brown adipocytes, and increased phosphoenolpyruvate carboxykinase (PEPCK) (*C*) and glycerol kinase (Gyk) (*D*) contents, as well as the gene expression of lipoprotein lipase (*Lpl*) and cluster of differentiation 36 (*Cd36*) (*E*) in BAT
Data are means ± SD; n = 6–12 rats. Student's t test was used to compare groups. *$P < 0.05$ *vs*. SC.

had reported reduced *in vivo* glucose utilization in BAT of rodent models of obesity (Ferré et al., 1986; Ishino et al., 2017; Lapa et al., 2017) and humans (Leitner et al., 2017; Orava et al., 2013), it was also possible that the uptake and oxidation of glucose would be impaired in these cells. Instead, our measurements of glucose uptake in isolated HFS BAT adipocytes revealed that it was significantly increased under both basal and insulin-stimulated conditions. This likely supported the elevated lactate production, indicating that glucose was being processed through the glycolytic pathway in these cells. Therefore, the α-glycerophosphate moiety necessary for enhanced FA esterification could be supplied in two ways: (1) by the formation of glycerol 3-phosphate as an intermediary step of glycolysis, and/or (2) through glyceroneogenesis. Because lactate is a major substrate for the latter pathway (Nye et al., 2008), its abundance also allowed for increased TAG synthesis. This was supported by elevated PEPCK content and confirmed by the enhanced incorporation of palmitate into TAG found in HFS BAT adipocytes. Additionally, because the content of GyK was increased in these cells, TAG synthesis from exogenous FA and glycerol was facilitated, which was also confirmed by significantly higher rates of glycerol incorporation into lipids in HFS than in SC BAT adipocytes. Lastly, with increased expression of *Lpl* and *Cd36*, the TAG content of BAT adipocytes could be enriched through the esterification of the abundant dietary fat carried by lipoproteins. In this context, less UCP1-mediated oxidation of glucose and fatty acids could be explained by a diversion of these substrates towards pathways of TAG synthesis as opposed to uncoupled oxidation. Altogether, these effects led to a reduction in the number of small lipid droplets and conferred a more unilocular appearance to adipocytes within BAT.

Interestingly, some adaptive responses of BAT adipocytes to the HFS diet (e.g. increased contents of PGC-1α, β3-AdR and CPT1B) were compatible with activation of a thermogenic response by these cells to overfeeding. This then begged the question why didn't this translate into increased UCP1-mediated substrate oxidation to support DIT? Importantly, we also found that content of TH, the rate-limiting enzyme for catecholamine biosynthesis, was markedly reduced in HFS BAT, indicating lower SNS-mediated recruitment of BAT activity. This is in line with our findings of reduced basal lipolysis in HFS BAT adipocytes, which could consequently lead to less UCP1 activation, even

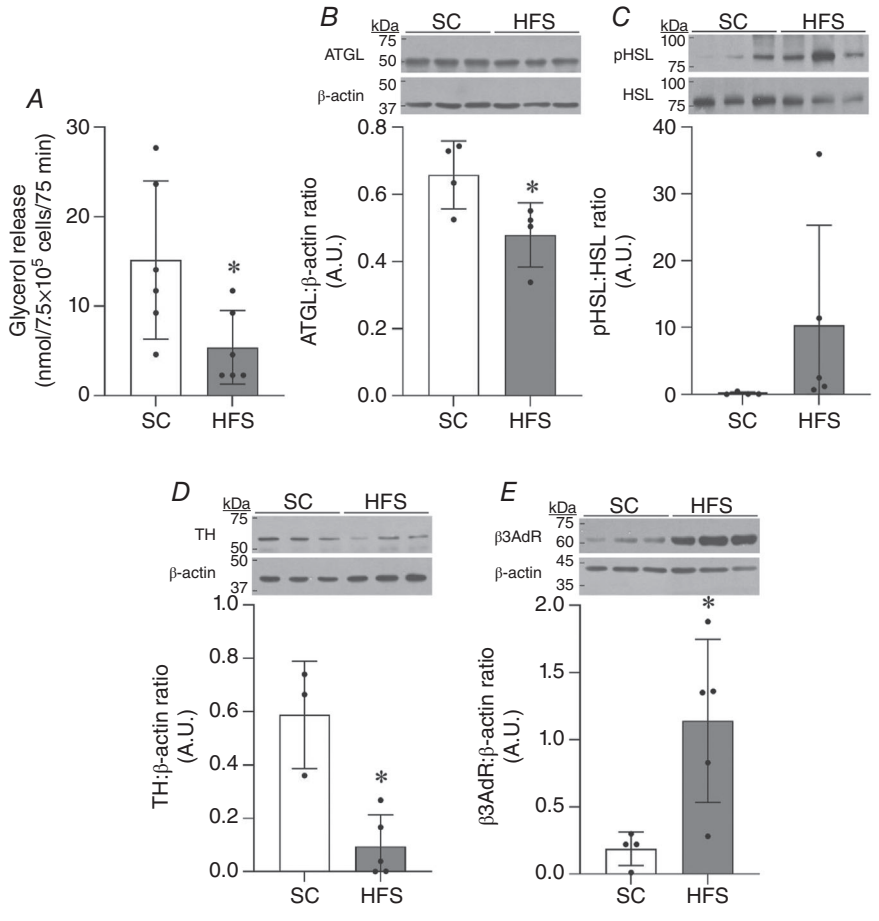

Figure 5. HFS diet reduced basal lipolysis (*A*) in isolated BAT adipocytes and the content of adipose triglyceride lipase (ATGL) (*B*), but did not signifiantly affect hormone sensitive lipase (HSL) phosphorylation (*C*). HFS diet also reduced tyrosine hydroxylase (TH) (*D*) and increased β3-adrenergic receptor (β3-Adr) (*E*) contents in BAT
Data are means ± SD; n = 3–6 rats. $^*P < 0.05$ *vs.* SC. Student's t test was used to compare differences between groups.

though the content of this protein and of others that support thermogenesis was increased. In this context, the increased content of β3-AdR we found in HFS BAT was likely a compensatory mechanism employed by the cell to maximize adrenergic activation, although, *in vivo*, it is futile given the drastic reduction in TH content and impaired catecholamine production in BAT of HFS rats. Thus, maintaining the ability of the SNS to promote UCP1 activation during prolonged HFS feeding seems to be crucial to sustain DIT and counteract weight gain. This is supported by previous studies reporting that basal sympathetic activation of BAT is reduced in rats chronically maintained on a high-fat diet (Levin et al., 1985; Madden & Morrison, 2016), and that diet-induced recruitment of BAT in mice depends essentially on sustained SNS-mediated activation (Fischer et al., 2019). Reduced SNS-mediated recruitment of BAT activity in HFS-induced obesity could originate from the development of leptin resistance. Indeed, rodent models of obesity lacking either functional leptin or a functional isoform of the leptin receptor display reduced SNS-mediated activation of BAT and DIT (Leibel et al., 1997; Leibel, 2008). Additionally, altered SNS activity (Levin et al., 1983) and reduced central leptin sensitivity (Levin & Dunn-Meynell, 2002) have been demonstrated in rats with diet-induced obesity. Therefore, it is likely that the molecular adaptations to the HFS diet we found in BAT originated from the diminished sympathetic output from the hypothalamus as a result of diet-induced leptin resistance (So et al., 2011). In fact, we have previously reported that plasma leptin levels of rats fed a HFS diet for 8 weeks were almost 2-fold higher than in SC diet-fed controls (So et al., 2011), indicating that these animals indeed had reduced sensitivity to this adipokine. However, because the production and release of leptin is proportional to WAT mass (Leibel, 2008), a gap exists between the beginning of HFS feeding and the time for adipose tissue to expand and leptin resistance to occur. This might be the reason why rats displayed increased whole-body energy expenditure in the first 2 weeks of high-fat feeding, and then lost this response afterwards (So et al., 2011) as leptin resistance developed. Thus, it could be that the increased UCP1 content in BAT we found after 8 weeks of a HFS diet was reminiscent of this initial DIT response mounted by the animal. Future studies are necessary to investigate this possibility.

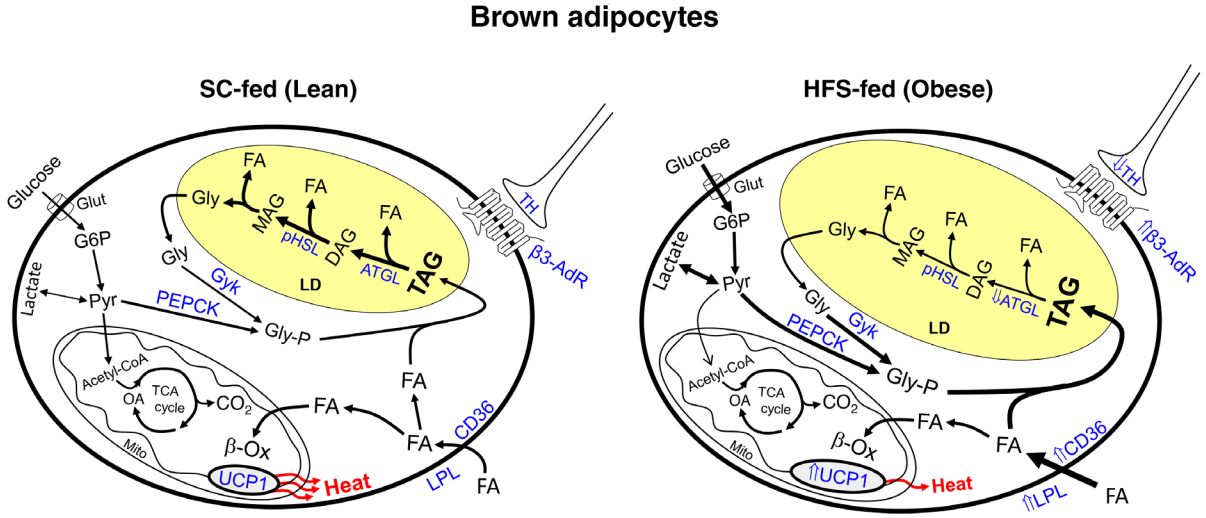

Figure 6. In brown adipocytes from lean rats fed a SC diet, glucose and fatty acids (FA) were diverted essentially toward UCP1-mediated substrate oxidation. These substrates were also used to sustain a high rate of triacylglycerol (TAG) breakdown/resynthesis. This was supported by a highly responsive molecular machinery that involved the activation of β3-adrenergic receptors (β3-AdR) via sympathetic nervous system-mediated release of noradrenaline and activation of the major lipolytic enzymes adipose triglyceride lipase (ATGL) and hormone sensitive lipase (HSL). Conversely, in BAT of rats fed a HFS obesogenic diet, despite increases in UCP1 and β3-AdR contents, substrate metabolism in BAT adipocytes was shifted toward TAG synthesis/storage. This was characterized by reduced UCP1-mediated glucose and fatty acid oxidation, impairment of lipolysis and reduction in tyrosine hydroxylase content in BAT. These adaptive responses to chronic HFS were supported by increased glucose uptake, contents of phosphoenolpyruvate carboxykinase (PEPCK) and glycerol kinase (GyK), elevated rates of glycerol incorporation into lipids and palmitate incorporation into TAG, and by enhanced gene expression of lipoprotein lipase (LPL) and cluster of differentiation 36 (CD36) in BAT
β-ox, β-oxidation; DAG, diacylglycerol; G6P, glucose-6-phospate; Glut, glucose transporter; Gly, glycerol; Gly-P, glycerol phosphate; LD, lipid droplet; MAG, monoacylglycerol; Mito, mitochondria; OA, oxaloacetate; Pyr, pyruvate. ⇑, increase; ⇓, reduction; thicker arrows indicate higher flow through the pathway. [Colour figure can be viewed at wileyonlinelibrary.com]

It is important to note that animals were housed at room temperature and not at thermoneutrality, which has been shown to have a significant impact on BAT UCP1 protein content and the contents of other mitochondrial proteins (McKie et al., 2019). This poses a potential limitation to our study as both groups of animals may have experienced BAT activation to some extent, which could have masked the effects of the diets. Moreover, the experiments in this study were conducted on male rats. Future studies assessing these parameters are warranted in female rats to identify sex-based differences, if any, in the adaptive responses of BAT to an obesogenic diet.

In summary, our findings provide novel evidence that increased BAT mass and its UCP1 content under chronic HFS feeding does not translate into elevated consumption of glucose or fatty acids through UCP1-mediated mitochondrial uncoupling. In fact, uncoupled glucose and fatty acid oxidation were even lower in HFS BAT adipocytes than in SC-fed controls after coupled respiration was inhibited in these cells by Oligo. Therefore, our findings are contrary to the idea that DIT is induced in brown adipocytes under conditions of diet-induced obesity. Rather, when an obesogenic high fat–sucrose-enriched diet was supplied for extended periods of time, brown adipocytes enhanced their ability to uptake and store glucose and FA, and did so by diverting substrate away from oxidation (Fig. 6). Collectively, these effects may impair BAT-induced DIT and likely contribute to the development of obesity and its related metabolic disorders.

References

Barbara, C., & Nedergaard, J. (2004). Brown adipose tissue: Function and physiological significance. *Physiological Reviews*, **84**, 277–359.

Cannon, B., & Nedergaard, J. (2001). Respiratory and thermogenic capacities of cells and mitochondria from brown and white adipose tissue. In G. Ailhaud (Ed.), *Adipose tissue protocols* (pp. 295–304). Humana Press Inc.

Dole, P. & Meinertz, H. (1960). Microdetermination of long-chain fatty acids in plasma and tissues. *Journal of Biological Chemistry*, **235**(9), 2595–2599.

Fedorenko, A., Lishko, P. V., & Kirichok, Y. (2013). Mechanism of fatty-acid-dependent UCP1 uncoupling in brown fat mitochondria. *Cell*, **151**(2), 400–413.

Feldmann, H. M., Golozoubova, V., Cannon, B., & Nedergaard, J. (2009). UCP1 ablation induces obesity and abolishes diet-induced thermogenesis in mice exempt from thermal stress by living at thermoneutrality. *Cell Metabolism*, **9**(2), 203–209.

Ferré, P., Burnol, A. F., Leturque, A., Terretaz, J., Penicaud, L., Jeanrenaud, B., & Girard, J. (1986). Glucose utilization *in vivo* and insulin-sensitivity of rat brown adipose tissue in various physiological and pathological conditions. *Biochemical Journal*, **233**(1), 249–252.

Fine, J. B., & DiGirolamo, M. (1997). A simple method to predict cellular density in adipocyte metabolic incubations. *International Journal of Obesity and Related Metabolic Disorders*, **21**(9), 764–768.

Fischer, A. W., Schlein, C., Cannon, B., Heeren, J., & Nedergaard, J. (2019). Intact innervation is essential for diet-induced recruitment of brown adipose tissue. *American Journal of Physiology. Endocrinology and Metabolism*, **316**(3), E487–E503.

Folch, J., Lees, M., & Sloane Stanley, G. H. (1957). A simple method for the isolation and purification of total lipides from animal tissues. *Journal of Biological Chemistry*, **226**(1), 497–509.

Gaidhu, M. P., Anthony, N. M., Patel, P., Hawke, T. J., & Ceddia, R. B. (2010). Dysregulation of lipolysis and lipid metabolism in visceral and subcutaneous adipocytes by high-fat diet: Role of ATGL, HSL, and AMPK. *American Journal of Physiology. Cell Physiology*, **298**(4), C961–C971.

Gaidhu, M. P., Fediuc, S., Anthony, N. M., So, M., Mirpourian, M., Perry, R. L. S., & Ceddia, R. B. (2009). Prolonged AICAR-induced AMP-kinase activation promotes energy dissipation in white adipocytes: novel mechanisms integrating HSL and ATGL. *Journal of Lipid Research*, **50**(4), 704–715.

Gaidhu, M. P., Fediuc, S., & Ceddia, R. B. (2006). 5-Aminoimidazole-4-carboxamide-1-beta-D-ribofuranoside-induced AMP-activated protein kinase phosphorylation inhibits basal and insulin-stimulated glucose uptake, lipid synthesis, and fatty acid oxidation in isolated rat adipocytes. *Journal of Biological Chemistry*, **281**(36), 25956–25964.

Gaidhu, M. P., Frontini, A., Hung, S., Pistor, K., Cinti, S., & Ceddia, R. B. (2011). Chronic AMP-kinase activation with AICAR reduces adiposity by remodeling adipocyte metabolism and increasing leptin sensitivity. *Journal of Lipid Research*, **52**(9), 1702–1711.

Ishino, S., Sugita, T., Kondo, Y., Okai, M., Tsuchimori, K., Watanabe, M., Mori, I., Hosoya, M., Horiguchi, T., & Kamiguchi, H. (2017). Glucose uptake of the muscle and adipose tissues in diabetes and obesity disease models: Evaluation of insulin and β3-adrenergic receptor agonist effects by 18F-FDG. *Annals of Nuclear Medicine*, **31**(5), 413–423.

Kozak, L. P. (2010). Brown fat and the myth of diet-induced thermogenesis. *Cell Metabolism*, **11**(4), 263–267.

Labbe, S. M., Caron, A., Bakan, I., Laplante, M., Carpentier, A. C., Lecomte, R., & Richard, D. (2015). In vivo measurement of energy substrate contribution to cold-induced brown adipose tissue thermogenesis. *FASEB Journal*, **29**(5), 2046–2058.

Lapa, C., Arias-loza, P., Hayakawa, N., Wakaba, H., Werner, A., Chen, X., Shinaji, T., Herrmann, K., & Pelzer, T. (2017). Whitening and impaired glucose utilization of brown adipose tissue in a rat model of type 2 diabetes mellitus. *Scientific Reports*, **7**(1), 16795.

Leibel, R. L. (2008). Molecular physiology of weight regulation in mice and humans. *International Journal of Obesity*, **32**(S7), S98-S108.

Leibel, R. L., Chung, W. K., & Chua, S. C. (1997). The molecular genetics of rodent single gene obesities. *Journal of Biological Chemistry*, **272**(51), 31937–31940.

Leitner, B. P., Huang, S., Brychta, R. J., Duckworth, C. J., Baskin, A. S., McGehee, S., Tal, I., Dieckmann, W., Gupta, G., Kolodny, G. M., Pacak, K., Herscovitch, P., Cypess, A. M., & Chen, K. Y. (2017). Mapping of human brown adipose tissue in lean and obese young men. *Proceedings of the National Academy of Sciences, USA*, **114**(32), 8649–8654.

Levin, B. E., & Dunn-Meynell, A. A. (2002). Reduced central leptin sensitivity in rats with diet-induced obesity. *American Journal of Physiology. Regulatory, Integrative and Comparative Physiology*, **283**(4), R941–R948.

Levin, B. E., Finnegan, M., Triscari, J., & Sullivan, A. C. (1985). Brown adipose and metabolic features of chronic diet-induced obesity. *American Journal of Physiology. Regulatory, Integrative and Comparative Physiology*, **248**(6), R717–R723.

Levin, B. E., Triscari, J., & Sullivan, A. C. (1983). Altered sympathetic activity during development of diet-induced obesity in rat. *American Journal of Physiology. Regulatory, Integrative and Comparative Physiology*, **244**(3), R347–R355.

Livak, K. J., & Schmittgen, T. D. (2001). Analysis of relative gene expression data using real-time quantitative PCR and the $2-\Delta\Delta CT$ method. *Methods*, **25**(4), 402–408.

Madden, C. J., & Morrison, S. F. (2016). A high-fat diet impairs cooling-evoked brown adipose tissue activation via a vagal afferent mechanism. *American Journal of Physiology. Endocrinology and Metabolism*, **311**(2), E287–E292.

McKie, G. L., Medak, K. D., Knuth, C. M., Shamshoum, H., Townsend, L. K., Peppler, W. T., & Wright, D. C. (2019). Housing temperature affects the acute and chronic metabolic adaptations to exercise in mice. *Journal of Physiology*, **597**(17), 4581–4600.

Nye, C. K., Hanson, R. W., & Kalhan, S. C. (2008). Glyceroneogenesis is the dominant pathway for triglyceride glycerol synthesis *in vivo* in the rat. *Journal of Biological Chemistry*, **283**(41), 27565–27574.

Olsen, J. M., Csikasz, R. I., Dehvari, N., Lu, L., Sandström, A., Öberg, A. I., Nedergaard, J., Stone-Elander, S., & Bengtsson, T. (2017). β 3-Adrenergically induced glucose uptake in brown adipose tissue is independent of UCP1 presence or activity: Mediation through the mTOR pathway. *Molecular Metabolism*, **6**(6), 611–619.

Orava, J., Nuutila, P., Noponen, T., Parkkola, R., Viljanen, T., Enerbäck, S., Rissanen, A., Pietiläinen, K. H., & Virtanen, K. A. (2013). Blunted metabolic responses to cold and insulin stimulation in brown adipose tissue of obese humans. *Obesity*, **21**(11), 2279–2287.

Rosenbaum, M., & Leibel, R. L. (1998). The physiology of body weight regulation: Relevance to the etiology of obesity in children. *Pediatrics*, **101**(Supplement_2), 525–539.

So, M., Gaidhu, M. P., Maghdoori, B., & Ceddia, R. B. (2011). Analysis of time-dependent adaptations in whole-body energy balance in obesity induced by high-fat diet in rats. *Lipids in Health and Disease*, **10**(1), 99.

Trayhurn, P. (2017). Origins and early development of the concept that brown adipose tissue thermogenesis is linked to energy balance and obesity. *Biochimie*, **134**, 62–70.

Wu, M. V., Bikopoulos, G., Hung, S., & Ceddia, R. B. (2014). Thermogenic capacity is antagonistically regulated in classical brown and white subcutaneous fat depots by high fat diet and endurance training in rats: Impact on whole-body energy expenditure. *Journal of Biological Chemistry*, **289**(49), 34129–34140.

Additional information

Data availability statement

All data supporting the results are included within the figures revealing their range and distribution.

Competing interests

The authors state no conflict or duality of interest with regards to this work.

Author contributions

Conception or design of the work: R.B.C. Acquisition, analysis or interpretation of data for the work: D.D.E. and S.J. Drafting the work or revising it critically for important intellectual content: D.D.E., S.J. and R.B.C. All authors have read and approved the final version of the manuscript and agree to be accountable for all aspects of the work in ensuring that questions related to the accuracy or integrity of any part of the work are appropriately investigated and resolved. All persons designated as authors qualify for authorship, and all those who qualify for authorship are listed.

Funding

This research was funded by a Discovery Grant from the Natural Science and Engineering Research Council of Canada (NSERC) and by infrastructure grants from the Canada Foundation for Innovation (CFI) and the Ontario Research Fund (ORF) awarded to R.B.C. D.D.E. was funded by NSERC Alexander Graham Bell Canada graduate scholarship-Doctoral.

Keywords

diet-induced thermogenesis, glyceroneogenesis, GyK, obesity, PEPCK, PGC-1α

Supporting information

Additional supporting information can be found online in the Supporting Information section at the end of the HTML view of the article. Supporting information files available:

Statistical Summary Document
Peer Review History